Revista de Teledetección. 2007. 27: 59-70

Detection of the urban heat-Island effect from a surface mobile platform

A. Jaschke Machado and T. Rezende de Azevedo
jaschke.machado@usp.br and xtarikx@usp.br

Laboratory of Climatology and Biogeography. University of São Paulo
Prof. Lineu Prestes Avenue, n 338, Cidade Universitária - Zip Code: 05508-000, São Paulo - Brazil

RESUMEN

Se ha medido la temperatura superficial de las calles estrechas, largas y profundas de la ciudad de Sao Paulo mediante el uso de termómetros infrarrojos de precisión (IRTs). Estos instrumentos van montados en una plataforma móvil, que se mueve por las calles. Los diagramas térmicos se determinaron a lo largo de transceptos sobre diferentes tipos de suelo y de ocupación del mismo, en las primeras horas del típico periodo nocturno de la estación seca. La temperatura del aire también se midió, junto con el flujo convectivo Q_H, entre la atmósfera y los edificios. La presencia de una isla de calor atmosférica alrededor del centro urbano se identificó bien, con un valor de 2ºC. Sobre la vertical parece que este fenómeno no es tan claro, aunque se detectó una oscilación térmica máxima de 6ºC entre las superficies más frías y la atmósfera.

PALABRAS CLAVE: Cartografía, áreas quemadas, MODIS, incendios, teledetección.

ABSTRACT

The surface temperature of the urban canyons in the city of São Paulo is remotely estimated through the use of precision infrared thermometers (IRTs). These instruments are set up on a mobile platform, which moves through the bottom of the canyons. The thermal patterns are verified, along a traverse, through the different kinds of soil coverage and occupation, during the early hours of a typical nocturnal period during the dry season. Air temperature measurements are also taken as well as estimates of the convective Q_H flux, between the atmosphere and urban buildings. The presence of an atmospheric urban heat island is well identified around the urban center, with a magnitude of 2°C. Over the vertical surface it appears that this phenomenon is not pronounced, although maximum thermal amplitude of around 6°C between the colder analyzed surfaces and the warmer atmosphere is identified.

KEY WORDS: mobile transect, surface temperature, urban, sensible heat.

INTRODUCTION

Geographical investigations in Brazil are currently undergoing a wide-ranging renewal process (MORAES, 2002). In terms of urban climate, tele-detective methods do not consist entirely of new frameworks; since the 80s orbital platforms have been being used to estimate, for example, patterns of surface heat islands. The use of a temporal series of meteorological variables to represent surface climate is also nothing new.

A new framework in field experiments consists of the utilization of mobile platforms over a surface and the indirect analysis of the patterns observed. These platforms can be mounted, in most cases, with tele-detection sensors, thermometers and radiometers that are sensitive to the infrared thermal band (between 8 and 14 μm). The results can show an interesting panorama of the simultaneous thermal processes that occur in time and space, and should be considered *a priori*.

The temporal and spatial variability, of the urban surface and the neighboring atmosphere temperatures, is a result of the complex exchange of energy fluxes through a volume containing this surface. In general, these fluxes are represented by a relationship of balance (OFFERLE *et al*. 2006) among the energy sources and sinks,

$$Q^* + Q_F = Q_H + Q_E + \Delta Q_S + \Delta Q_A + S \qquad (1)$$

Q_F and Q^*, respectively, represent the anthropogenic and natural energy sources. The natural sources are derived from the net radiative processes

which come from solar energy and atmospheric emission. However, this determination is complex, especially in the case of the long wave radiative fluxes, where what are anthropogenic and what are natural observed parcels is not evident. In the canopy layer the term Q* can turn up a sink or a source of energy, and a direct relationship with the period of the day is never possible.

Q_H and Q_E represent the turbulent exchanges of energy, by convection, between the surface and the air. They are defined, respectively, by a sensible and a latent component.

By defining a volume that concerns the interface between the surface and the atmosphere (OKE, 1988), the term ΔQ_S indicates the variability of storage energy in this volume and is mainly associated to the sink of energy by conduction. On the other hand, ΔQ_A represents the variability of energy advected among physically distinct regions.

As the balance energy expressions are only an idealized representation of the inherent complexity of the environmental energy exchanges, the term S indicates the fluxes that are still not parameterized, for example: the removal of the surface energy by varying types of water runoff, the accumulated and dissipated photosynthetic energy of the vegetative processes, and also the various manners in which energetic materials are stored.

The observed thermal patterns in the city of São Paulo are complex, not only because of the complexity of the urban surface, but also due to the seasonal climatic variability. The tropical climate in the region of São Paulo has an annual variability which is well defined between the dry and wet seasons. Yet, it can show daily thermal amplitudes higher than the annual average thermal amplitude. This characteristic makes it so that the estimates of terms in the energy balance (MORAES *et al.,* 1977; MACHADO and AZEVEDO, 2007), have to be even done more precisely. A more detailed description of the spatial distribution of temperatures must include the types and the geographical orientations of the surfaces.

Temperature fields observed by remote sensors installed in orbital platforms are not always adjusted for effects caused by the relative orientation to the surfaces targeted (SOUX *et al*., 2004). Many times, it is necessary to validate them in respect to surface observations. In other cases, the moisture quantities on the surface should be reported (SPRONKEN-SMITH *et al.,* 2000), especially when urban parks are investigated.

A more comprehensive spatial distribution of the temperatures in urban areas can be reached using mobile transects over the surface (VOOGT and OKE, 1997; VOOGT and OKE, 1998; MACHADO and AZEVEDO, 2005). In these transects the air temperature and the wall temperatures of the urban canyons are usually observed. These investigations can be teledetective, in a like manner to the orbital platforms. Then, it is possible to use infrared thermometers (IRTs) over vehicles in displacement on the streets. The apparent surface temperatures that are observed must be adjusted (WITTICH, 1997) to the emissions effects.

Oke (1987) indicates that these procedures of measurement can lead to a maximum error of between 1°C and 2°C, when no adjustments are made. Because the observed target is generally placed near the vehicle, the atmospheric effect is reduced considerably. The main sources of error are due to surface emissivity and sensor precision. In the case of micro-scale experiments, the use of IRTs is more satisfactory if the vision field is reduced more in respect to the target (MASSON *et al.,* 2002).

In the analysis presented here of the metropolitan region of São Paulo, a period of two hours following sunset, with a night of clear skies, during the dry season, and under calm conditions was chosen. This episode denotes the transition between the daily and the nocturnal period of an atypical Friday, because there was an extended weekend due to a four-day vacation. However, it is possible to verify the dynamic of the thermal environment and its spatial distribution.

The atmospheric urban heat-island effect is verified, and now it must be related to the city's population. In order to compare the results of this paper with those obtained for other cities, it is worthwhile to mention that the official population of the city of São Paulo is 10,434,252 inhabitants (PMSP, 2000). If the Metropolitan Area of São Paulo is considered , the population is 17,878,703 inhabitants (PMSP, 2000).

INSTRUMENTS AND METHODS

Calculate of the energy balance terms

The thermal state of a volume between the surface and the atmosphere is defined by the balance among the various energy fluxes (Eq. 1) that pass through this volume.

In the inside of this volume there is a boundary that represents the interface between the surface and the atmosphere. Because of its irregular shape, it is very difficult to determine this boundary, which is defined by one or a combination of the following: public routes, urban vegetation, the grass or impermeable canopies, or the walls and roofs of the buildings. Understanding the exchange of energy is also complicated, because this surface is made up of widely varying elements (i) that also cover a large variety of areas (ai), with differing dimensions.

Some energetic fluxes rising from this surface are related to turbulent energetic, or convective, exchanges. They are directly related to the physical properties of the atmosphere, such as temperature (Ta), vapor pressure (ea), the psychrometric constant (γ), density (ρ) and the air's specific heat (cP) in relation to the constant pressure, as well as being related to surface properties, like temperature (Ti) and vapor pressure (ei).

Next, the energetic fluxes that are currently being investigated and estimated are presented in terms of their physical-mathematical representation and integrality over a variety of surfaces types. They represent, respectively, the natural energetic sources, or net radiation (Q*), anthropogenic energy sources (QF), turbulent convection by sensible heat (QH), turbulent convection by latent heat (QE), variability in storage energy (ΔQS), variability in advected energy (ΔQA) and various energetic sinks (S) related to surface water runoff, photosynthesis and other as yet unexplored sinks:

$$Q^* = \Sigma\, a_i\, Q^*_i \quad (2)$$

$$Q_F = \sum a_i\, Q_{fi} \quad (3)$$

$$Q_H = \sum a_i\, \rho\, c_P\, (T_i - T_a) \quad (4)$$

$$Q_E = \sum a_i\, \rho\, c_P\, (e_i - e_a) / \gamma \quad (5)$$

$$\Delta Q_S = \sum a_i\, \Delta Q_{si} \quad (6)$$

$$\Delta Q_A = \sum a_i\, \Delta Q_{ai} \quad (7)$$

$$S = \sum a_i\, S_i \quad (8)$$

It must be noted that Q* can still be specified in terms of the radiation fluxes of short wave (K), and long wave (L). These fluxes are represented just as much by the direction from which they reach any surface (K$\downarrow$ e L$\downarrow$), located above the reference surface. Alternatively, they are represented as the direction from which they are irradiated or emitted to the atmosphere (or another surface kind) from the reference surface being considered (K$\uparrow$ e L$\uparrow$):

$$Q^* = (K\downarrow - K\uparrow) + (L\downarrow - L\uparrow) \quad (9)$$

On the other hand, the radiation fluxes can also be represented using this same notation basis. By considering the Stefan-Boltzmann constant (σ) and the radiation proprieties of the various types of surfaces (including the atmosphere), such as albedo (α) and emissivity (ε), it is possible to obtain the incoming solar radiation (K$\downarrow$), reflected solar radiation (K$\uparrow$), incoming thermal radiation (L$\downarrow$) and emitted thermal radiation (L$\uparrow$), respectively:

$$K\downarrow = \sum ai\, K\downarrow i \quad (10)$$

$$K\uparrow = \sum ai\, (1 - \alpha i)\, K\downarrow i \quad (11)$$

$$L\downarrow = \sum ai\, L\downarrow i \quad (12)$$

$$L\uparrow = \sum ai\, \varepsilon i\, \sigma\, Ti4 \quad (13)$$

Data Acquisition

The material used in the field experiment, to analyze the spatial distribution of the temperature was gathered with the following equipment:

- A Micro Logger Campbell Scientific Inc. (CSI), model CR3000, serial number 1189, with 14 channels and two rechargeable acid batteries of 9 V.
- Two infrared Apogee thermometers, IRT precision model; both are sensitive to the spectral band between 6.0 μm and 14.0 μm. Serial numbers 2061 and 2065, respectively, with a vision angle of around 20º and a response time of 1 second.
- A RM Young temperature sensor (connected to a ventilated tube), RTD model, serial number TS11222; sensitive to a thermal amplitude between -50 °C and +50ºC.

During this procedure, a platform (Fig. 1) was mounted over a Ford, Escort Hobby, vehicle. This vehicle is used as a sort of mobile laboratory, with the instruments attached to the platform (Fig. 1b).

All traverses performed with the mobile platform were geo-referenced through simultaneous use of a manual geo-positioning system: GPS12 model from GARMIN.

Preliminary sensitivity tests were carried out to verify the sensors' performance. These preliminary results were compared to values obtained in previous experiments (MACHADO and AZEVEDO, 2005) in similarly occupied areas.

Regarding the displacement of the mobile laboratory, a mean velocity of around 30kmh^{-1} was reached. Higher velocities damage the spatial resolution that it is necessary for the analysis, and a lower velocity generates traffic problems on the streets.

The data were sampled at a frequency of 0.5 Hz and were stored in one minute, corresponding to 30 observed values. There is no exact definition in respect to the spatial resolution, because it depends of the velocity. Considering a temporal resolution of 1minute for stored data, and a mean displacement velocity of around 30 kmh^{-1}, a mean spatial resolution of around 500m is reached. But, in terms of a temporal resolution of 2 seconds for the sampled data, and the same displacement velocity, a spatial resolution of 15m is reached.

In situations where there is more intensive traffic, using the same temporal resolutions, but with a mean velocity of around 40 kmh^{-1}, the spatial resolution falls, and a stored resolution of around 700m and a sampled resolution of around 20m is collected. In opposing situations, using the same temporal resolutions, but with a mean velocity of around

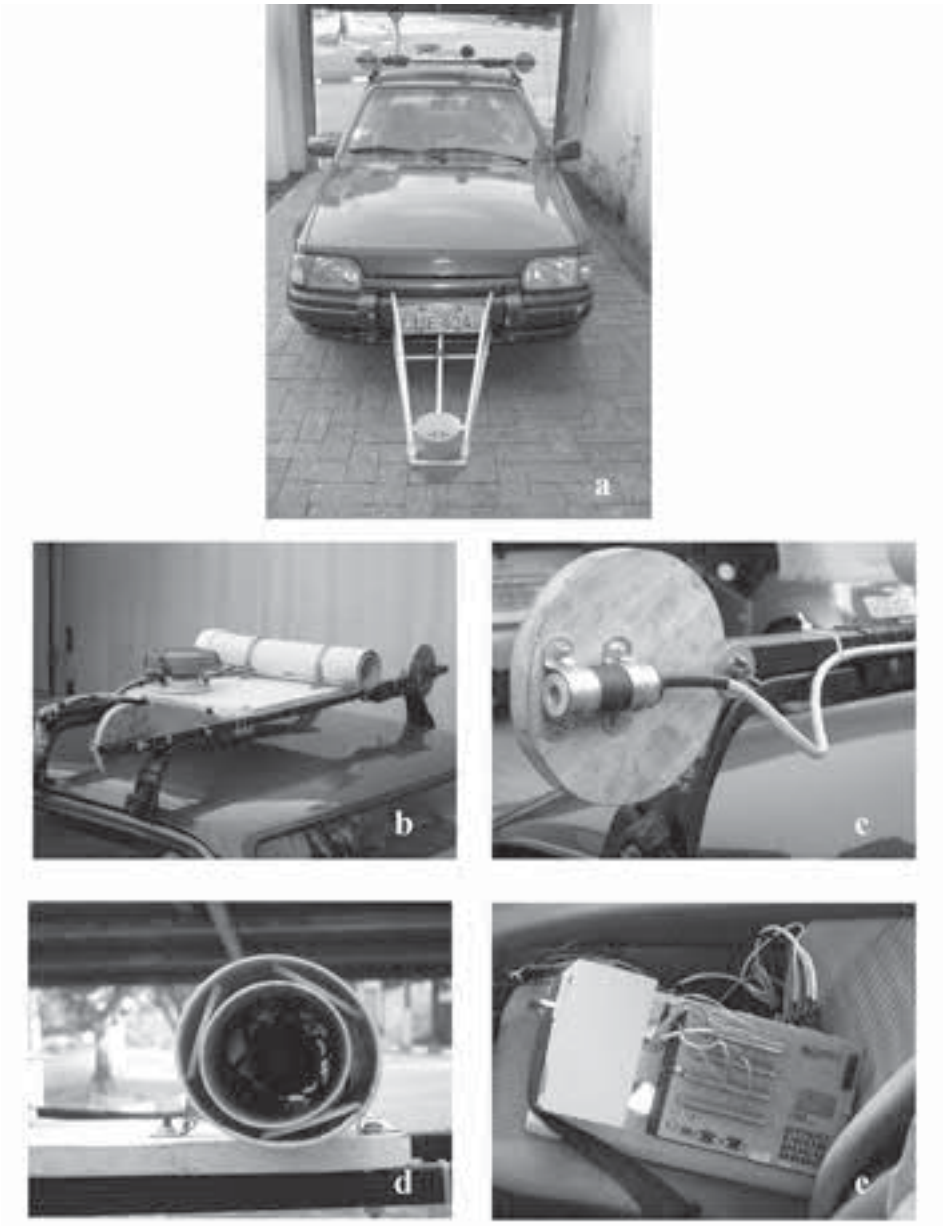

Figura 1. Mobile laboratory (a) and platform (b), with the IRT sensors attached to rotational discs (c) and the RTD sensor attached to a ventilated tube (d). All sensors are connected to a data acquisition system (e) inside the vehicle. The acquired data are geopositioned by using a GPS manual that is that is also situated inside of the vehicle.

20 kmh^{-1}, the spatial resolution increases to 300m and 10m, respectively.

Scalar analysis of the study area

The analysis was performed on a traverse in the city of São Paulo, through the use of the mobile laboratory. This experiment is based on the scalar climate perspective (Tab. 1) (MONTEIRO, 1975; ORLANSKI, 1976). By taking the obtained temporal and spatial scales into consideration, this experiment is notable for being capable of including both phenomena of the micro scale α and the meso scale γ.

Estimate of the adjustment for the apparent surface temperature

The measurements taken with the IRTs sensors, made by Apogee Instruments and sold by Campbell Scientific Instruments (CSI), are linearly adjusted to obtain the value closest to the real surface temperature (T_i).

From the apparent temperature (T_{ap}) recognized by the thermocouple precision sensor, to the thermal infrared channel, installed inside the instrument body, a set of three coefficients (P, H and K) are applied. These coefficients correspond to three installed thermocouples and are related through a second order polynomial to the temperature of the instrument. A reference temperature for the estimates is also needed.

The air temperature taken with the RTD sensor was used as a reference temperature. Then, as with other procedures that use infrared sensors (MACHADO and AZEVEDO, 2006), the thermal equilibrium can be reached in mobile measurements.

Based on these considerations, the following correction is applied to obtain the target temperature:

$$T_i = T_{ap} - \frac{0.25}{P}.[(T_{ap} - H)^2 - K] \qquad (14)$$

$>10^4$ km	stability waves	tide waves				Macro α
10^4 km - 2.000 km		baroclinic waves				Macro β
2.000 km - 200 km		fronts and hurricanes				Meso α
200 km - 20 km			Instability lines and breezes			Meso β
20 km - 2 km			thunderstorms and **urban**	**effects**		Meso γ
2 km - 200 m				tornades and seek convection		Micro α
200 m - 20 m				eddies and	thermals	Micro β
< 20 m					plumes and turbulence	Micro γ
	> 1 month	month - day	day - hour	hour - min	min - sec	

Table 1. Orlanski's representation of the meteorological phenomena and their relative association to the urban climatic effects. The following concepts are indicated: Orlanski's theory (solid), empirical (solid and horizontal lines) and Monteiro's theory (solid, horizontal and diagonal lines). The empirical scale corresponds to the temporal and spatial scales obtained with the mobile laboratory.

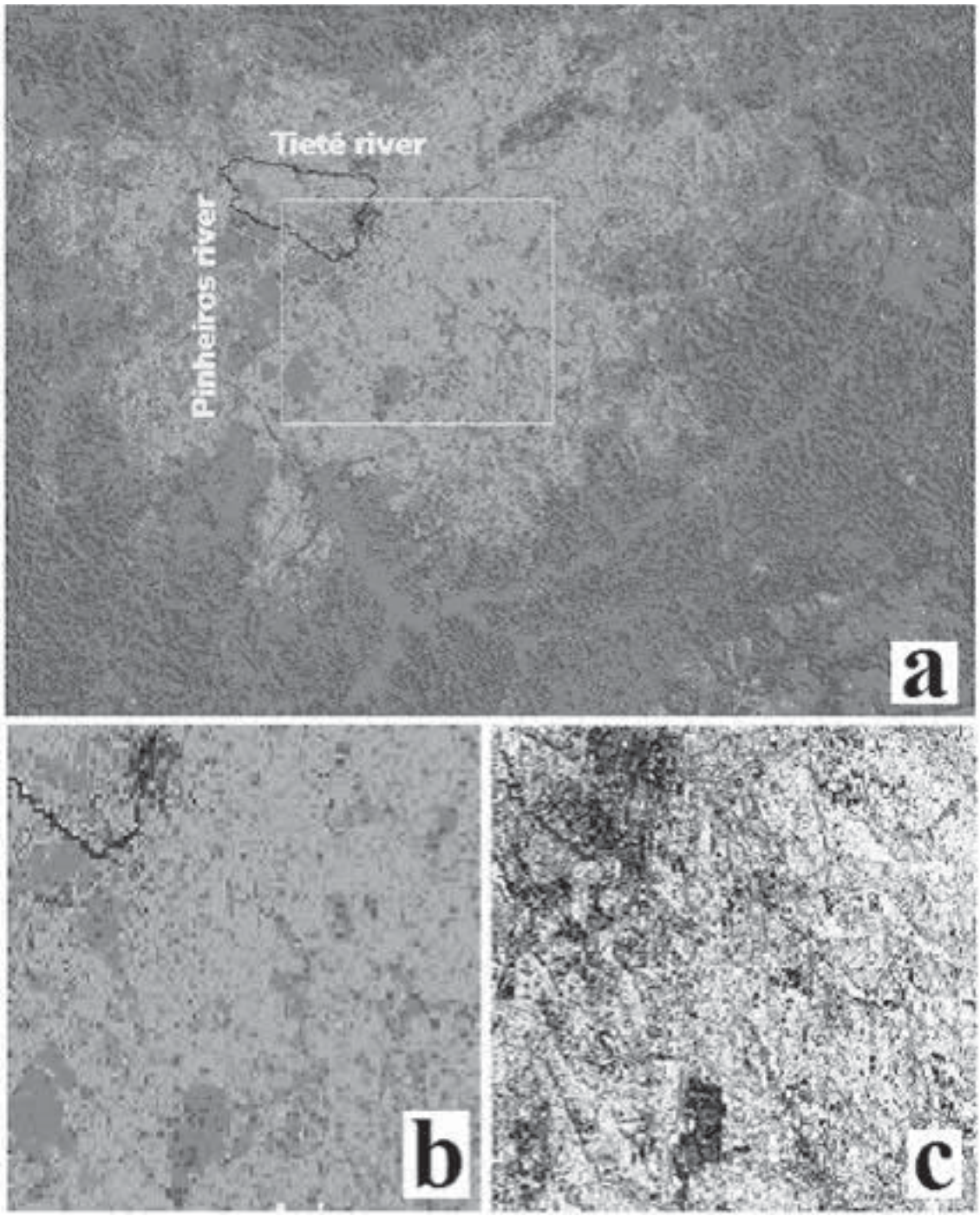

***Figure 2.** Soil occupation classification of the Metropolitan Area of São Paulo, basded on Q* estimates (a): external suburban (dark green), internal suburban (light green), urban (light gray), dense urban (dark gray) and water surfaces (blue). The red polygonal represents the traverse. The area delimited by the yellow polygonal square has been amplified (b) and compared to the image obtained from the estimated surface albedo(c). The light gray tones (c) indicate the highest albedo values, while the dark tones indicate the shortest values. Some important locations are indicated in blue (c). It can be seen that the high density building area (c-above) and a densely vegetated area (c - below) present low albedo values.

Todas las figuras precedidas de asterisco se incluyen en el cuadernillo anexo de color

For a better understanding of the results, it must be noted that the temperature accuracy of the Apogees radiometers is specified at around 0.3°C from -10° to 55°C (CAMPBELL and APOGEE, 2005, p. 1). But, when a sensor body and target are at the same temperature, there is a lower error of around 0.1°C. Therefore, during cloudy or nocturnal experiments, when temperature of the surface does not vary greatly, the margin of error will be lower than under sunny conditions.

Final classification

Finally, the obtained results and the traverse are analyzed from the perspective of soil occupation. A soil classification showed by Machado and Azevedo (2007) of the São Paulo metropolitan region is considered when comparing the albedo estimate obtained by the Lopes (2003) method, using images of the Landsat channels. The soil occupation classification considers the existence of five categories: inner urban, external urban, inner suburban, external suburban and water surfaces. This classification is done from the perspective of the surface magnitude of Q* estimated for the city of São Paulo.

RESULTS AND DISCUSSION

A traverse (Fig. 2a) in the inner urban region of the city of São Paulo is done, crossing the central, densely urbanized area and also the neighboring area of a large urban park. A segmented image of the Q* estimates (Fig. 2b), which includes a sector of the traverse, is compared to the same segmented area in the image obtained from the surface albedo estimates (Fig. 2c).

Surface albedo corresponds to the parcel of K↓ that is reflected (K↑). The calculation was done with consideration of the visible channels (1 to 3), and the near infrared (4) and the middle infrared (5 and 7) from the LANDSAT, according to the procedure used by Lopes (2003) in the city of Lisbon. The modal value obtained for the metropolitan area of São Paulo, including the densely urbanized region and the suburban region, was 0.22. Considering the averaged value of 0.25 and a sample interval of 90%, it was observed that the typical albedo for the city of São Paulo corresponds to an interval between 0.17 and 0.31. It is interesting to note that the densely urbanized region shows much higher albedo values than the treed areas or the water surfaces, between 0.25 and 0.30, while the urban core, with high concentrations of buildings, shows more reduced values similar to the treed areas, varying between 0.15 and 0.20 (Fig. 2c).

The temperature patterns of the air and the canyons' walls (Figs 3b) were observed through the traverse. The main traverse corresponds to a polygonal figure compound of approximately three consecutive shorter traverses (Fig. 3a), in the west-east, north-south and southeast-northwest directions, respectively. The wall temperatures are estimated and adjusted using the IRT sensors. The adjustment of the apparent temperature uses the sampled air temperature as a reference temperature. When the target was too far from the sensor, the wall temperature was approximated to the air temperature.

Due to the nocturnal cooling and to the total traverse period (Δt), there is a negative tendency (Fig. 3b), approximately linear, associated with the higher scale (mesoγ) that must be removed in order to procedure to the shorter scale analysis (microα). This tendency can be filtered out by adding the observed temperatures to the verified half-amplitude (ΔT) between opposite sampled points, in (t) moments of the same period around the median instant of the total traverse, and based on the final amplitude resulting in the initial (T_{start}) and the final ($T_{arrival}$) observed temperatures:

$$\Delta T = (T_{start} - T_{arrival}).\frac{(t-1)}{\Delta t} - \frac{(T_{start} - T_{arrival})}{2} \quad (15)$$

By observing the temperature profiles, it is possible to detect some of the patterns associated to distinct soil occupations. The presence of a heat island, with maximum amplitude around 2ºC (Fig. 3c), in the intermediate sector of the traverse is evident. This sector corresponds to the north-south traverse through the central region of the city.

The wall temperature patterns indicate systematic behavior of variable amplitudes (Fig. 3c), between the temperatures on the walls opposite the observed canyons. Both traverses, west-east, north-south, and southeast-northwest show this pattern, respectively, because of the increased width of the canyon, the geographical position of the walls in relation to the sun at the end of the afternoon and the presence of an urban park on a lateral of the canyon.

On the other hand, if the spatial distribution is represented (Fig. 4), a more realistic thermal pat-

tern, better defined in terms of soil occupation, is observed. Other adjustments are also possible. For example, at the beginning of the total traverse, a more elevated amplitude (Figs. 3c and 4b) is merely a result of the thermal evolution in the location where the instruments were mounted. It is also noted that the observed atmospheric heat island is not situated exactly over the central core of the city. Its maximum amplitude is positioned over an intermediary region, between a large avenue running along the Tietê River and the citiy's central area.

Analysis of the wall temperatures can also be done in terms of their geographical positioning. From the total traverses (Fig. 3a) certain sectors were selected, where the displacement direction was oriented approximately according to the east-west and north-south directions (Fig. 5). But, as the principal axis of the streets and avenues do not correspond exactly to these directions, the sectors of the traverses where the displacement direction had a maximum difference of 30° in respect to the reference directions were then considered.

In the east-west displacements (Fig. 5a) a well defined pattern can be seen, especially along the avenue running along the Tietê. Curiously, the south faces show lower temperatures than the north faces. Along the north-south displacements (Fig.

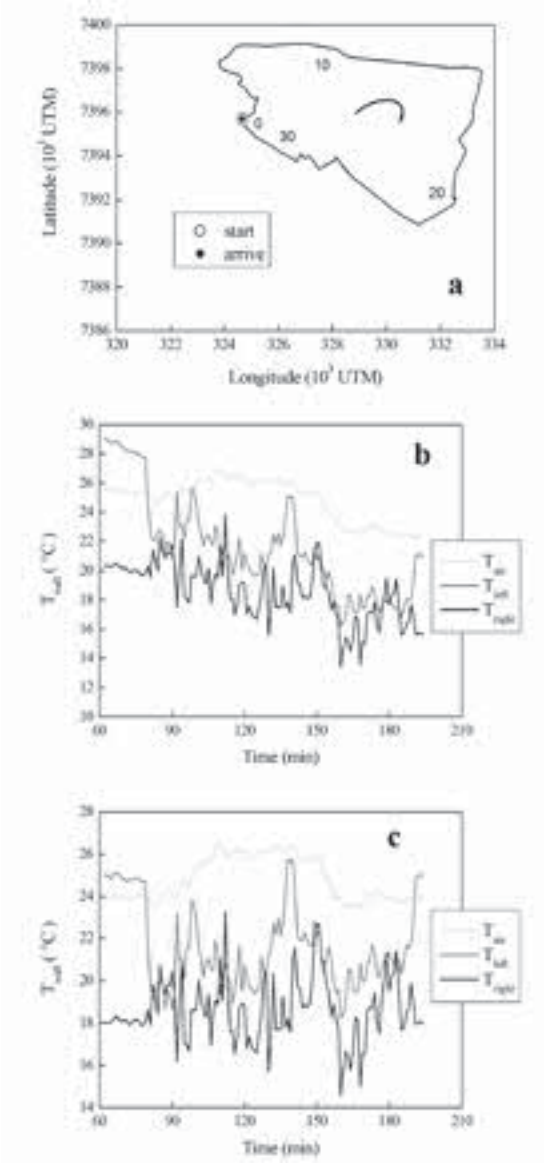

Figure 3. Geo-positioned traverse (a), with the coinciding start and arrival positions. The decimal positions in kilometers are indicated from the initial position. The evolution of the air and wall temperatures (b) and their respective projections around the mean values (c) is verified according to the entire traverse. This projection is obtained by applying the adjustment proposed in Equation 15, which filters nocturnal cooling.

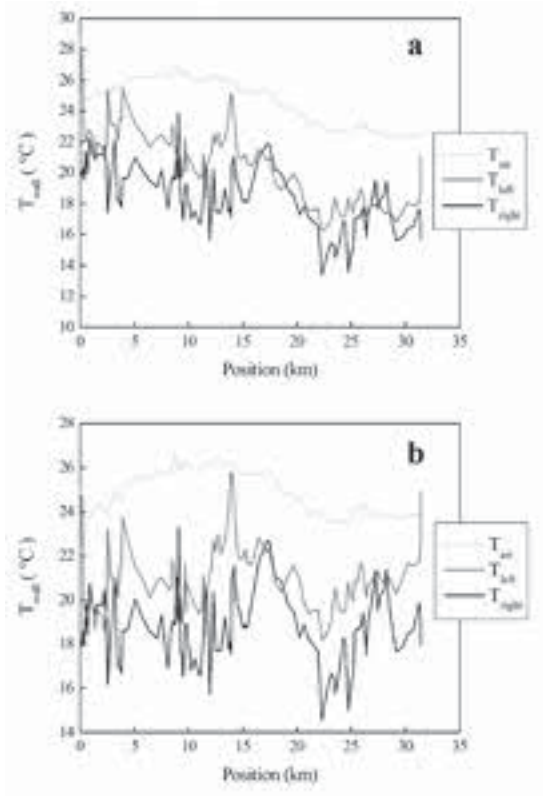

Figure 4. Ditto for Figures 3b and 3c, which replace the temporal evolution with the spatial distribution. Here the GPS information registered is associated to the simultaneous obser-ved flux.

5b) there is not a generally well defined pattern, except in the sector near the city's central area. In this direction the prevailing observations show that the east faces are warmer than the west faces. This is logical because the information was gathered at the beginning of the nocturnal period. During the hours before the experiment, the east faces were just under the solar radiation.

By taking the specific heat of the dry air (c_p) and its density (ρ) in the city of São Paulo, (around 10^{-3} $J.kg^{-3}.C^{-1}$ and 925 $g.m^{-3}$ respectively), into consideration and through application of Equation 4 to the mean profile of the observed temperatures (Fig. 3c and Fig. 4b), in addition to using the mobile averages in consecutive intervals of ten minutes, it is possible to estimate the profile of the turbulent flux of sensible heat between the atmosphere and the walls of the canyons (Fig.6).

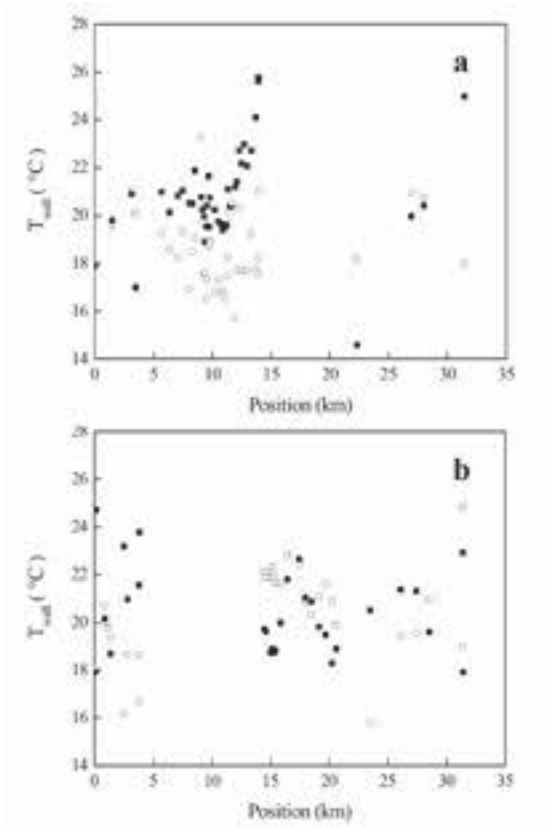

Figure 5. Spatial distribution of the wall temperatures in the sectors with east-west (a) and north-south (b) displacements. The white symbols indicate the walls facing the north or the west, while the black symbols indicate the walls facing the south or the east. The circles represent the information gathered with the sensor positioned on the right side of the vehicle, while the squares represent the information gathered with the other sensor positioned on the left side. The black symbols corre-spond to the warmer targets, because of the relative solar disk position during the afternoon period.

In almost the entire complete traverse the sensible heat is negative, indicating that there is an energy sink in the urban volume. This energy sink is directed at the buildings' surfaces, which are cooling faster than the atmosphere. An observed maximum intensity of this energy flux (Fig. 6b) can also be seen around the area corresponding to the maximum atmospheric heat island observed (Fig. 4b).

Adjustment for emissivity could easily be done (CASELLES et al., 1991; VALOR et al., 2000), by an effective emissivity. But the propose of this paper it is to show a conservative estimate of QH. Preliminary tests were performed using the typical emissivity of walls (OKE, 1978), from 0.71 to 0.95. Variability in temperature, caused by an emissivity effect ranging from 0.3° to 1.8°C, was observed. However, there is still not a precise survey, on this scale, of the emissivity values for the city of São Paulo.

Experimental studies, and the models based upon them, do not allow for the separation of the effects of the geometrical features from the anthropometric features (GIVONI, 1998). But, in the experiment here presented, the atmospheric urban heat-island effect is placed in an area of a very low height/width ratio. And, the traverse is placed in the metropolitan area. The heat-island is shown to be an adjustment effect of the geometrical and the anthropogenic features.

Adjustment for emissivity could easily be done (CASELLES et al., 1991; VALOR et al., 2000), by an effective emissivity. But the propose of this paper it is to show a conservative estimate of QH. Preliminary tests were performed using the typical emissivity of walls (OKE, 1978), from 0.71 to 0.95. Variability in temperature, caused by an emissivity effect ranging from 0.3° to 1.8°C, was observed. However, there is still not a precise survey, on this scale, of the emissivity values for the city of São Paulo.

Experimental studies, and the models based upon them, do not allow for the separation of the effects of the geometrical features from the anthropometric features (GIVONI, 1998). But, in the experiment here presented, the atmospheric urban heat-island effect is placed in an area of a very low height/width ratio. And, the traverse is placed in the metropolitan area. The heat-island is shown to be an adjustment effect of the geometrical and the anthropogenic features.

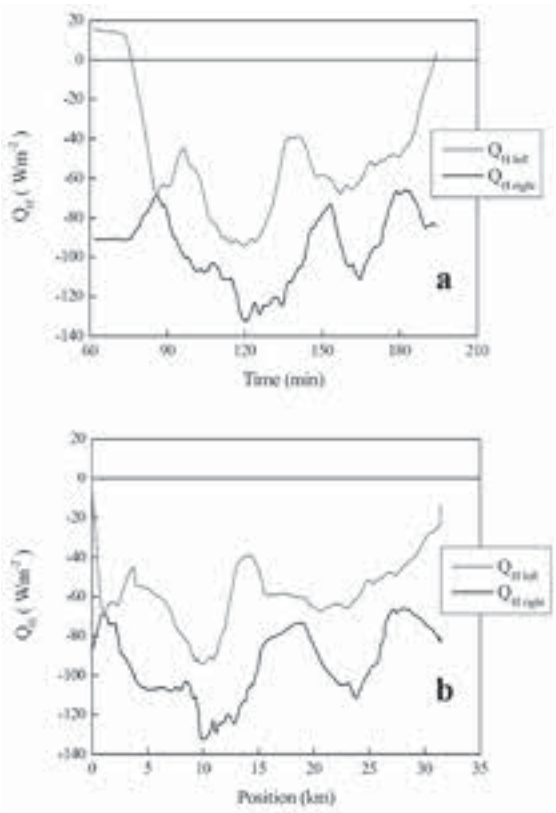

Figure 6. The temporal evolution (a) and the spatial distribu-tion (b) of the sensible heat flux estimated for the urban surface canyons of the city of São Paulo, at the beginning of the noc-turnal period on a typical day during the dry season. Eq.4 is used for every ten mobile averaged values from Figure 4, with the initially observed high amplitude (a) being caused by a specific situation when the vehicle was parked.

CONCLUSIONS

Remote temperature detection of urban elements, from a mobile platform on the surface, is shown to be a useful framework for describing thermal patterns. Some energy fluxes, such as the long wave radiation flux and the sensible heat convective flux, can be estimated and contribute to the validity of satellite observations.

Observations of urban areas, that have sectors with distinct soil occupation types, can be useful for estimating the proportion of fluxes directly associated with anthropogenic activities.

It is worthwhile to note that the mobile experiment demonstrated was done under calm conditions, in relation to the atmospheric dynamic. In unstable meteorological systems the observed conditions could be decreased and the thermal gradients drastically reduced.

But, under stable atmospheric conditions, and taking the local climatic seasonality into consideration, it would be possible to determine some stability and energy partitioning parameters such as, for example, the Richardson number and the Bowen ratio. Along these lines, the turbulent sensible heat flux estimates could lead to estimates of the latent component related to turbulent exchanges.

The geo-morphological and topographic aspects could also constitute an additional effect to be analyzed, when using this method of estimation and observation of the fluxes. Initially, the effects generated by the different soil cover and occupations are considered. But, because of the terrain topography, some adjustment may be necessary under very pronounced declivities.

The mean atmospheric heat island observed, with a magnitude value of around 2°C at the beginning of the nocturnal period, is not equally apparent from observations of the surface temperatures. However, this is a relevant effect, because it can contribute to the generation of an intra-urban breeze pattern in the city of São Paulo. This possible pattern can also occur in other sectors of the city's greater metropolitan area, if there is a soil occupation similar to the one observed here.

The real positioning of the observed phenomena in this experiment, was only possible because, besides observation of the physical properties through the traverse, the geo-references of the observed magnitudes were also sampled. Following which, it was apparent that the heat island is placed over an area with shorter buildings than the central core of the city, but closer to an important expressway, where there is an obviously high displacement of vehicles. Among these vehicles are buses and trucks, which emit polluted gases contributing to the greenhouse effect.

The wall temperatures seem to correspond well to solar warming at the end of the diurnal period, in relation to their geographical positioning. This is more evident for streets following the north-south direction. However, for streets following the east-west direction the same effect is not confirmed. It is true that the maximum solar incidence observed on a north facing wall (southern hemisphere) occurs around the midday. But it must be considered that the Tietê Avenue, running along the banks of the Tiete River, is not exactly an urban canyon, becau-

se the height/width ratio between the building and street dimensions, respectively, is very low. Therefore, since vehicle displacement was close to the right side of the avenue, and the left IRT sensor was quite far from the target, it is possible that the temperatures of the south facing walls could have been overestimated. Because the air reference temperature was, in general, higher than the wall temperatures in this sector of the total traverse.

During the start of the nocturnal period, the atmospheric temperature is still around 6°C (Fig. 3c) warmer than the building surfaces, in a conservative estimate for the nocturnal period, when the emissivity adjustment is not applied. In the city's central region, this temperature gradient generates an estimated turbulent sensible heat flux superior to 100 Wm^{-2} (Fig. 4). This means that after sunset thermal turbulence can be a significant phenomena that may contribute, in the nocturnal period, to the dissipation of the atmospheric heat island's stored energy to the cooler urban cover, which is susceptible to the loss of energy by the long wave radiation emissions.

ACKNOWLEDGMENTS

This paper received support from FAPESP (Research Assistance Foundation of the State of São Paulo), process number 05/56287-0. Antonio Jaschke Machado received a doctoral scholarship from CNPq-Brazil (National Council of Scientific and Technological Development) while researching this paper.

BIBLIOGRAPHIC REFERENCES

CAMPBELL Scientific, Inc. and APOGEE Instruments, Inc. (2005) Instruction manual: IRTS-P Precision Infrared Temperature Sensor. CSI, Logan/Utah, USA, 12 p.

CASELLES, V.; LÓPEZ GARCÍA, M. J.; MELIÁ, J. and PÉREZ CUEVA, A. J. (1991) Analysis of the heat-island effect of the city of Valencia, Spain, through air temperature transects and NOAA satellite data. Theoretical and Applied Climatology, 43, 195-203.

GIVONI, B. (1998) Climate considerations in building and urban design. New York, John Wiley & Sons, Inc., 464 p.

LOPES, A. M. S. (2003) *Modificações no clima de Lisboa como conseqüência do crescimento urbano*. Doctoral Thesis in Physical Geography, University of Lisbon, 360 p (in Portuguese).

MACHADO, A. J. and AZEVEDO T. R. (2007) *A distribuição espacial dos termos do balanço de energia em superfície a partir de imagem orbital e observação de campo*. In: *Revista do Departamento de Geografia* (accepted in January). University of São Paulo (in Portuguese).

MACHADO, A. J. and AZEVEDO T. R. (2006) *A necessidade de correção das medidas de radiação térmica obtida através de plataformas móveis em áreas urbanas*. In: III *Seminário de Pesquisa em Geografia Física - SEPEGE*, December 11 and 12, 37-48, São Paulo, (in Portuguese).

MACHADO, A. J. and AZEVEDO T. R. (2005) *Fluxo diurno de radiação de onda longa recebida em um trajeto urbano arborizado*. In: *XI Simpósio Brasileiro de Geografia Física Aplicada - Geografia, Tecnociência, Sociedade e Natureza*. São Paulo, 100-109 (in Portuguese).

MASSON, V., GRIMMOND C. S. B. and OKE T. R. (2002) Evaluation of the Town Energy Balance (TEB) scheme with direct measurements from dry districts in two cities. Journal of Applied Meteorology, 41, 1011-1026.

MONTEIRO, C. A. F. (1975) *Teoria e Clima Urbano*. Thesis, *Faculdade de Filosofia, Letras e Ciências Humanas*. University of São Paulo (in Portuguese).

MORAES, A. C. R. (2002) *Geografia: pequena história crítica*. *Hucitec Editorial, São Paulo*, 138p (in Portuguese).

MORAES, A. C. R.; COSTA W. M. da and TARIFA J. R. (1977) *Tipos de tempo e balanço de energia na cidade de São Paulo*. *In*: *Climatologia*, 8, Institute of Geography, FFLCH/USP, São Paulo (in Portuguese).

OFFERLE, B.; GRIMMOND C. S. B.; FORTUNIAK K.; KLYSIK K. and OKE T. R. (2006) Temporal variations in heat fluxes over a northern European city centre. Theoretical and Applied Climatology, 84, 103-115.

OKE, T. R. (1988) The urban energy balance. Progress in Physical Geography, 12,47-508.

OKE, T. R. (1987) Street design and urban canopy layer climate, Energy and Buildings, 11, 103-113.

OKE, T. R. (1978) Boundary Layer Climates. Methuen & Co Ltd, London, 372 p.

ORLANSKI, I. (1976). A simple boundary condition for unbounded hyperbolic flows. Journal of Computational Physics, 21, 251-269.

PMSP - *Prefeitura do Município de São Paulo* (2000)
http://www.capital.sp.gov.br/portalpmsp (in Portuguese).

SOUX, A.; VOOGT, J. A. and OKE, T. R. (2004) A model to calculate what a remote sensor 'sees' of an urban surface. Boundary-Layer Meteorology,111 (1), 109-132.

SPRONKEN-SMITH, R. A.; OKE, T. R. and LOWRY, W. P. (2000) Advection and the surface energy balance of an irrigated urban park. International Journal of Climatology, 20, 1033-1047.

VALOR, E.; CASELLES, V.; COLL, C.; SÁNCHEZ, F.; RUBIO, E. y SOSPEDRA, F. (2000) *Análisis comparativo del efecto de isla térmica de la ciudad de Valencia con imágenes TM, MUST y AVHRR. Revista de Teledetección, 14, 5-10* (in Spanish).

VOOGT, J.A. and OKE, T. R. (1998) Radiometric temperatures of urban canyon walls obtained from vehicle traverses, Theoretical and Applied Climatology, 60, 199-217.

VOOGT, J.A. and OKE, T. R. (1997) Complete Urban Surface Temperatures. Journal of Applied Meteorology, 36 (9), 1117-1132.

WITTICH, K. P. (1997) Some simple relationships between land-surface emissivity, greenness and the plant cover fraction for use in satellite remote sensing. International Journal of Biometeorology, 41, 58-64.